Tetraoxaporphycene: ESR/ENDOR, UV/Visible/Near-IR, and MO-Theoretical Study of Its Five Redox Stages

Rainer Bachmann,[†] Fabian Gerson,*[,†] Georg Gescheidt,[†] and Emanuel Vogel[‡]

Contribution from the Institut für Physikalische Chemie der Universität Basel, Klingelbergstrasse 80, CH-4056 Basel, Switzerland, and Institut für Organische Chemie der Universität zu Köln, Greinstrasse 4, D-50939 Köln 41, Germany

Received July 6, 1993[⊗]

Abstract: The radical cation ($3^{\bullet+}$), radical anion ($3^{\bullet-}$), and dianion (3^{2-}) of tetraoxaporphycene were generated from the neutral compound (**3**) and the dication (3^{2+}). The two paramagnetic species, $3^{\bullet+}$ and $3^{\bullet-}$, give rise to highly resolved ESR spectra, which have also been investigated by ENDOR and TRIPLE-resonance spectroscopy. The ion pairs formed by the radical anion $3^{\bullet-}$ with alkali-metal counterions become less tight when the size of the cation increases from Li^+ through Na^+ and K^+ to Cs^+. Proton, ^7Li, ^{23}Na, ^{39}K, and ^{133}Cs hyperfine data are consistent with the structure of the ion pairs, in which the counterion is situated on the 2-fold axis above or below the molecular plane. The absorption spectra of all five redox stages in the UV/visible/near-IR region (300–950 nm) and the emission bands of the three diamagnetic species are similar to those of the isomeric and isoelectronic tetraoxaporphyrins, 4^{2+}–4^{2-}, which have recently been investigated. The absorption bands were assigned to electronic transitions with the use of PPP (Pariser–Parr–Pople) calculations. Bond-length alternation along the 20-membered π-perimeter is predicted by theory for the neutral compound **3**, in accord with the NMR spectra and the X-ray structural data. In the dication 3^{2+}, the four oxygen atoms should bear one positive π-charge, which is largely preserved in the consecutive reduction stages, as additional electrons are almost exclusively accommodated by the perimeter.

Introduction

Porphycene (**1**), an isomer of porphyrin (**2**),[1] was synthesized several years ago.[2] Later, workers from the same laboratory reported the isolation of the perchlorate salt of the tetraoxaporphycene dication (3^{2+}), in which the NH groups and N atoms of the parent **1** are replaced by O and O^+, respectively.[3] The radical anions of **1** and some of its alkyl derivatives have been characterized by their hyperfine data with the use of ESR, ENDOR, and TRIPLE-resonance spectroscopy.[4] Furthermore, the UV/visible spectra of both **1** and the isoelectronic dication 3^{2+} have been studied thoroughly by experiment and theory.[5]

Here, in addition to 3^{2+}, we report on the corresponding radical cation $3^{\bullet+}$, the neutral compound **3**, the radical anion $3^{\bullet-}$, and the dianion 3^{2-}, which are isoelectronic with the free base porphycene (**1**), its radical anion $1^{\bullet-}$, and the (hitherto unknown) further reduction stages, 1^{2-}, $1^{\bullet 3-}$, and 1^{4-}, respectively. They are both isoelectronic and isomeric with the five analogous redox stages, 4^{2+}, $4^{\bullet+}$, **4**, $4^{\bullet-}$, and 4^{2-}, of tetraoxaporphyrin, which were recently investigated in detail,[6] after the perchlorate salt of the dication 4^{2+} and the unstable neutral compound **4** (tetraoxaisophlorin) had been isolated.[7]

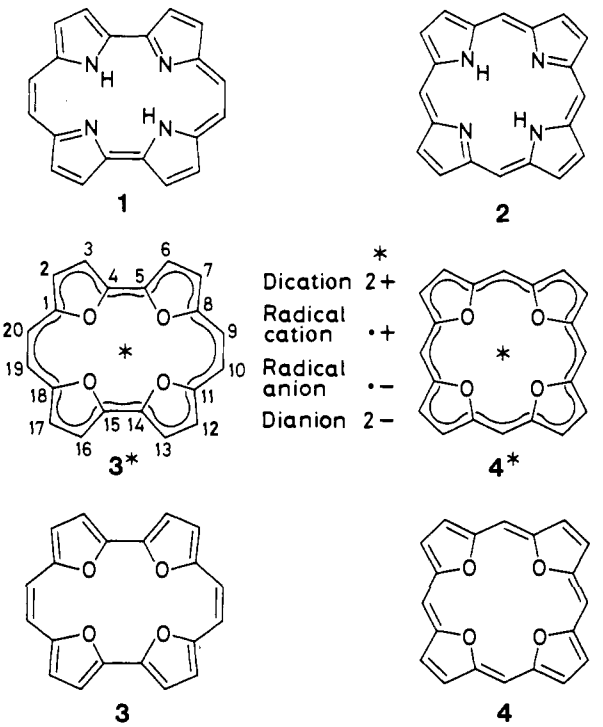

The essential structural difference between 4^{2+} and 3^{2+} is the lowering of symmetry from D_{4h} to D_{2h}. Consequently, in contrast to 4^{2+}, the lowest vacant orbitals of 3^{2+} are nondegenerate and so is the ground state of the radical ions $3^{\bullet+}$ and $3^{\bullet-}$. Whereas the ESR lines of $4^{\bullet+}$ and $4^{\bullet-}$ are extremely broad and resistant to saturation,[6] the radical cation $3^{\bullet+}$ and the radical anion $3^{\bullet-}$

[†] Universität Basel.
[‡] Universität zu Köln.
[⊗] Abstract published in *Advance ACS Abstracts*, October 1, 1993.

(1) *The Porphyrins*; Dolphin, D. J., Ed.; Academic Press: New York, 1978/1979; Vols. I–VII.
(2) Vogel, E.; Köcher, M.; Schmickler, H.; Lex, J. *Angew. Chem., Int. Ed. Engl.* **1986**, *25*, 257. Vogel, E.; Köcher, M.; Balci, M.; Teichler, I.; Lex, J.; Schmickler, H.; Ermer, O. *Angew. Chem., Int. Ed. Engl.* **1987**, *26*, 931. Wehrle, B.; Limbach, H.-H.; Köcher, M.; Ermer, O.; Vogel, E. *Angew. Chem., Int. Ed. Engl.* **1987**, *26*, 934. Aramendia, P. F.; Redmond, R. W.; Nonell, S.; Schuster, W.; Braslawsky, S. E.; Schaffner, K.; Vogel, E. *Photochem. Photobiol.* **1986**, *44*, 555. Ofir, H.; Regev, A.; Levanon, H.; Vogel, E.; Köcher, M.; Balci, M. *J. Phys. Chem.* **1987**, *91*, 2686. Vogel, E. *Pure Appl. Chem.* **1990**, *62*, 557.
(3) Vogel, E.; Sicken, M.; Röhrig, P.; Schmickler, H.; Lex, J.; Ermer, O. *Angew. Chem., Int. Ed. Engl.* **1988**, *27*, 411.
(4) Schlüpmann, J.; Huber, M.; Toporowicz, M.; Plato, M.; Köcher, M.; Vogel, E.; Levanon, H.; Möbius, K. *J. Am. Chem. Soc.* **1990**, *112*, 6463.
(5) Waluk, J.; Müller, M.; Swiderek, P.; Köcher, M.; Vogel, E.; Hohlneicher, G.; Michl, J. *J. Am. Chem. Soc.* **1991**, *113*, 5511.
(6) Bachmann, R.; Gerson, F.; Gescheidt, G.; Vogel, E. *J. Am. Chem. Soc.* **1992**, *114*, 10855.
(7) Vogel, E.; Haas, W.; Knipp, B.; Lex, J.; Schmickler, H. *Angew. Chem., Int. Ed. Engl.* **1988**, *27*, 406. Röhrig, P. Ph.D. Thesis, Universität zu Köln, 1991.

0002-7863/93/1515-10286$04.00/0

Scheme I

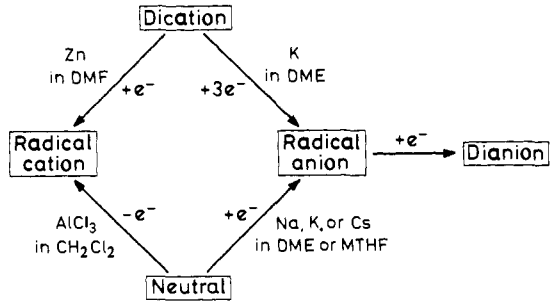

give rise to highly resolved ESR spectra which can readily be saturated. In the present work, this feature has enabled us to study $3^{\bullet+}$ and $3^{\bullet-}$ not only by ESR but also by ENDOR and general-TRIPLE-resonance spectroscopy. Particularly, ion pairs formed by $3^{\bullet-}$ with various alkali-metal counterions have systematically been investigated. UV/visible/near-IR spectra are presented for all five redox stages, 3^{2+}, $3^{\bullet+}$, **3**, $3^{\bullet-}$, and 3^{2-}, along with their interpretation by the aid of PPP (Pariser–Parr–Pople) calculations, which also provide π-bond orders and π-charge populations in these species.

Experimental Section

The synthesis of the tetraoxaporphycene dication (3^{2+}) perchlorate and its precursor, the neutral O-bridged [20]annulene (**3**), was described previously.[3] Methods of preparation of the three remaining redox stages $3^{\bullet+}$, $3^{\bullet-}$, and 3^{2-} from 3^{2+} or **3** are indicated in Scheme I. The radical cation $3^{\bullet+}$ was generated at ambient temperature by reduction of 3^{2+} with zinc in *N,N*-dimethylformamide (DMF) or by oxidation of **3** with $AlCl_3$ in dichloromethane. The radical anion $3^{\bullet-}$ was produced by reaction of **3** at 195 K with sodium, potassium, or cesium in 1,2-dimethoxyethane (DME) or 2-methyltetrahydrofuran (MTHF). In the case of sodium and cesium, the metallic mirror was formed by decomposition of the corresponding azide. Further contact of the solution with the alkali metal at 195 K yielded the dianion 3^{2-}. Both $3^{\bullet-}$ and 3^{2-} could also be obtained by prolonged reaction of 3^{2+} with potassium in DME at low temperature. The counterion Li^+ was introduced by addition of LiCl salt in excess to solutions of $3^{\bullet-}$ prepared from **3** with potassium in DME or MTHF. The ESR spectra of $3^{\bullet+}$ and $3^{\bullet-}$ were taken on a Varian-E9 spectrometer, while a Bruker-ESP-300 system served for ENDOR and TRIPLE-resonance investigations.

The UV/visible/near-IR studies of 3^{2+} and **3** were performed on their solutions in concentrated sulfuric acid and DME, respectively, whereas those of $3^{\bullet+}$, $3^{\bullet-}$, and 3^{2-} had to be carried out on the reaction mixtures, in which these species were generated (see above). The optical cell was attached to the evacuated vessel together with an ESR tube, so that the progress of the oxidation or reduction could be monitored by formation or decay of the paramagnetic stages. Electronic absorption spectra were taken at ambient temperature on Hewlett-Packard 8452A diode array (UV/visible) and Perkin-Elmer Lambda-9 (near-IR) instruments. The corresponding emission bands (uncorrected) were registered on a Spex-Fluorolog/Spex-Datamate spectrometer.

Results and Discussion

ESR/ENDOR Spectra: Radical Cation. Figure 1 shows the ESR spectrum of the radical cation $3^{\bullet+}$ generated from the neutral compound **3** with $AlCl_3$ in dichloromethane ($g = 2.0024 \pm 0.0001$). An identical spectrum is observed upon reduction of the dication 3^{2+} with Zn in DMF (Scheme I). Analysis of the fully resolved hyperfine pattern yields, in a straightforward way, three coupling constants ($a_{H\mu}$), each for a set of four equivalent protons: 0.169, 0.145, and 0.123 mT (experimental error, ±0.001 mT). This analysis has been confirmed by observation of the three pertinent pairs of proton-ENDOR signals (not reproduced here) and by computer simulation of the ESR spectrum (Figure 1). A general-

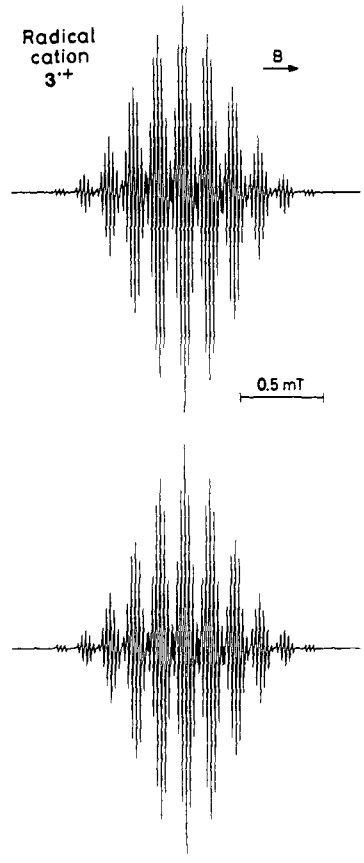

Figure 1. (Top) ESR spectrum of the radical cation, $3^{\bullet+}$, of tetraoxaporphycene in dichloromethane; temperature, 273 K. (Bottom) Simulation with the use of the proton coupling constants, $a_{H\mu}$, given in the text and Table I; line shape, Lorentzian; line width, 0.009 mT.

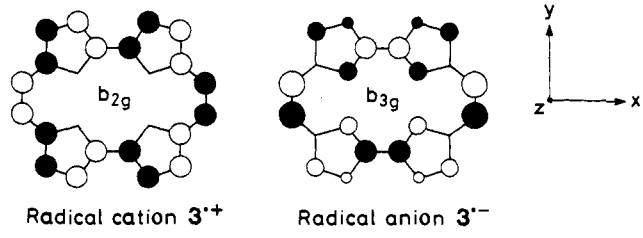

Figure 2. Diagrams of the HOMO (b_{2g}) and LUMO (b_{3g}) of tetraoxaporphycene (**3**), which are singly occupied in the radical cation $3^{\bullet+}$ and the radical anion $3^{\bullet-}$, respectively, as calculated in the frame of the Hückel–McLachlan procedure.

TRIPLE-resonance experiment[8] performed on these signals indicates that all three $a_{H\mu}$ values have the same sign, which is certainly negative, as required for protons directly attached to π-centers μ (α-protons).[9a]

The singly occupied orbital of $3^{\bullet+}$ (b_{2g} in the D_{2h} symmetry) can be considered as a "pure" annulene MO, because it has nodes at the four oxygen atoms (Figure 2). The Hückel–McLachlan procedure,[10] with the use of standard heteroatom parameters[11] and $\lambda = 1.0$, gives $\rho_\mu = +0.051 \pm 0.001 \approx {}^1/_{20}$ as the π-spin population at each of the carbon centers of the 20-membered

(8) Kurreck, H.; Kirste, B.; Lubitz, W. *Electron Nuclear Double Resonance Spectroscopy of Radicals in Solution*; VCH Publishers: New York, 1988; Chapter 2.

(9) See, for example: Gerson, F. *High-Resolution ESR Spectroscopy*; Wiley, Verlag Chemie: New York, Weinheim, 1970; (a) Chapter 1.5; (b) Appendix A.2.2.

(10) McLachlan, A. D. *Mol. Phys.* **1960**, *3*, 233.

(11) $\alpha_O = \alpha + h_O\beta$ and $\beta_{CO} = k_{CO}\beta$ with $h_O = 1.5$–2.0 and $k_{CO} = 0.8$; see, for example: Streitwieser, A., Jr. *Molecular Orbital Theory for Organic Chemists*; Wiley: New York, 1961; Chapter 5.2. Because of the nodes at the four oxygen atoms in b_{2g} (Figure 2), the π-spin populations ρ_μ in $3^{\bullet+}$ do not significantly depend on the choice of h_O.

Table I. Proton Coupling Constants, $a_{H\mu}$ (in mT), for the Radical Cation, $3^{\bullet+}$, of Tetraoxaporphycene, as Compared to Those of the Isoelectronic Radical Anion, $1^{\bullet-}$, of Porphycene

μ	$1^{\bullet-}$ [a]	$3^{\bullet+}$
2, 7, 12, 17	−0.146	−0.145
3, 6, 13, 16	−0.180	−0.169
9, 10, 19, 20	−0.095	−0.123

[a] From ref 4.

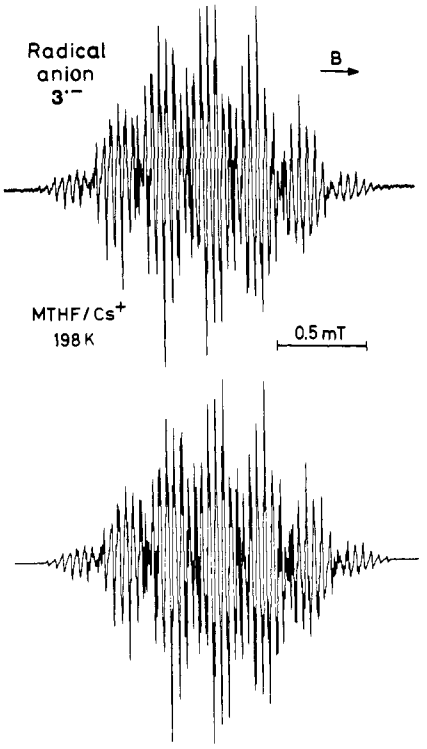

Figure 3. (Top) ESR spectrum of a tightly ion paired radical anion, $3^{\bullet-}$, of tetraoxaporphycene. Solvent, counterion, and temperature are as indicated. (Bottom) Simulation using the proton and ^{133}Cs coupling constants, $a_{H\mu}$ and a_{Cs}, given in Table II; line shape, Lorentzian; line width, 0.012 mT.

perimeter. This ρ_μ value converts into $a_{H\mu} = -0.143 \pm 0.003$ mT for all 12 perimeter protons, when the McConnell equation,[12] $a_{H\mu} = Q\rho_\mu$, is applied to it with the proportionality factor $Q = -2.8$ mT. The procedure thus leads to a general agreement with experiment, but assignments of the coupling constants $a_{H\mu}$ to the three sets of four protons in individual positions μ of $3^{\bullet+}$ are not feasible, in view of the near equality of the calculated π-spin populations ρ_μ. However, such assignments can be made by comparison of the hyperfine data for $3^{\bullet+}$ with those of the isoelectronic radical anion, $1^{\bullet-}$, of porphycene,[4] as indicated in Table I.

ESR/ENDOR Spectra: Radical Anion. Depending on the strength of association with its counterion, Li^+, Na^+, K^+, or Cs^+ (ion pairing), the ESR spectra of the radical anion $3^{\bullet-}$ are of two types ($g = 2.0032 \pm 0.0001$ throughout). Diagnostic in this respect is the appearance of an additional hyperfine splitting from the nucleus, ^7Li, ^{23}Na, ^{39}K, or ^{133}Cs, of the counterion.[9b] The ESR spectra exhibiting such a splitting are considered to arise from *tight* ion pairs of $3^{\bullet-}$ and M^+ (M = Li, Na, K, or Cs), and those lacking it are regarded as due to *loose* ones. The two types of spectra are exemplified in Figures 3 and 4. In MTHF, tight ion pairs are exclusively formed in the whole temperature range of investigation (183–298 K). In DME, with higher cation-solvating power, cooling of the solution from 298 to 198 K leads to a change

(12) McConnell, H. M. *J. Chem. Phys.* **1956**, *24*, 632.

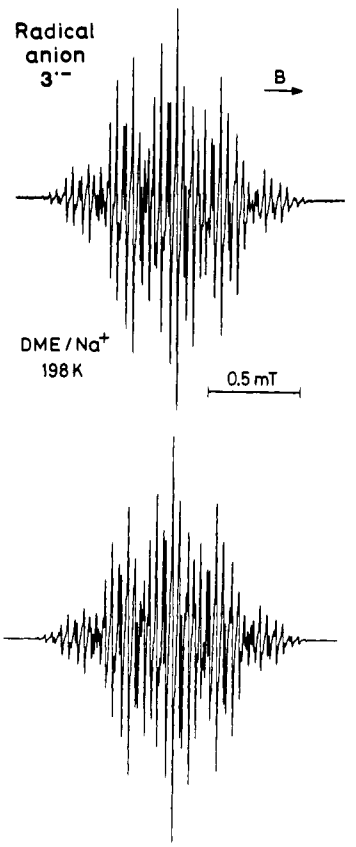

Figure 4. (Top) ESR spectrum of a loosely ion paired radical anion, $3^{\bullet-}$, of tetraoxaporphycene. Solvent, counterion, and temperature are as indicated. (Bottom) Simulation using the proton coupling constants, $a_{H\mu}$, given in Table II; line shape, Lorentzian; line width, 0.012 mT.

of tight into loose ion pairs, the range of temperature in which this transformation occurs varying somewhat for particular counterions.

Coupling to ^7Li, ^{23}Na, or ^{133}Cs nuclei is also manifest in the ENDOR spectra of the tight ion pairs which exhibit signals from these nuclei along those from protons. Not detected are the corresponding signals from ^{39}K nuclei, because they fall below 1 MHz, the frequency limit of our ENDOR system. As an illustration, Figure 5 shows the ENDOR spectra of the tight ion pairs formed by $3^{\bullet-}$ with Li^+ and Cs^+ in MTHF. General-TRIPLE experiments carried out on such spectra indicate that the coupling constants of the ^7Li, ^{23}Na, and ^{133}Cs nuclei, a_{Li}, a_{Na}, and a_{Cs}, have the same negative sign as the $a_{H\mu}$ values of the 12 α-protons. This statement should also hold for the ^{39}K coupling constants, a_K, in which case no such experiment was practicable. Under the conditions, where additional splittings from alkali-metal nuclei are observed, the coupling constants of these nuclei (a_{Li}, a_{Na}, a_K, and a_{Cs}) did not markedly depend on the temperature.

The hyperfine data for the tight and loose ion pairs of the radical anion $3^{\bullet-}$ and its counterions are listed in Table II. Assignments of the coupling constants $a_{H\mu}$ to sets of four protons in the individual positions μ are based on the results of Hückel–McLachlan calculations ($\lambda = 1.0$).[10] In contrast to the singly occupied orbital of the radical cation $3^{\bullet+}$ (b_{2g}), the corresponding orbital of $3^{\bullet-}$ (b_{3g}) has substantial LCAO coefficients at the four oxygen atoms, and the π-spin distribution over the 20 carbon centers μ of the perimeter is less even (Figure 2). To account for the enhanced electron demand by the four oxygen atoms in $3^{\bullet-}$, as a consequence of the association with the counterion, a higher value of the parameter h_O[11] was adopted for the tight than for the loose ion pairs. The change in h_O from 2.0 to 1.5, on going from the former to the latter, causes the π-spin populations ρ_μ at μ = 2, 7, 12, 17 and at 3, 6, 13, 16 to decrease from +0.035 and +0.018 to +0.031 and +0.011, respectively, and those at 9,

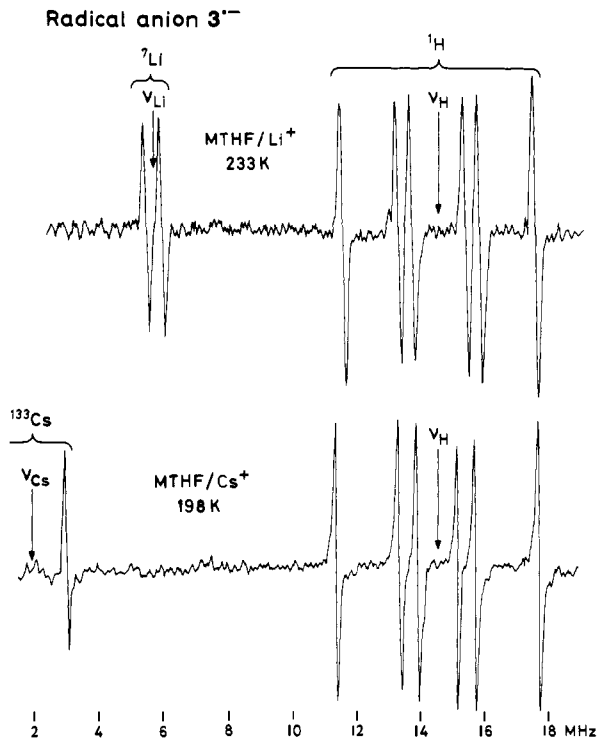

Figure 5. Proton-, ^{7}Li-, and ^{133}Cs-ENDOR spectra of tightly ion paired radical anions, $3^{\bullet-}$, of tetraoxaporphycene. Solvent, counterion, and temperature are as indicated.

Table II. Coupling Constants of Protons and Alkali-Metal Nuclei, $a_{H\mu}$ and a_M (in mT),[a] for the Radical Anion, $3^{\bullet-}$, of Tetraoxaporphycene

		tight ion pair[b]				loose ion pair[c]
		Li^+	Na^+	K^+	Cs^+	
$a_{H\mu}$; μ =	2, 7, 12, 17	−0.091	−0.087	−0.085	−0.085	−0.085
	3, 6, 13, 16,	−0.060	−0.050	−0.047	−0.043	−0.037
	9, 10, 19, 20	−0.215	−0.221	−0.223	−0.228	−0.234
a_M		−0.019	−0.030	−0.009	−0.076	

[a] M = Li, Na, K, or Cs. Experimental error: ±0.001 mT. [b] Solvent, MTHF; temperature, 198 K. [c] Solvent, DME; temperature, 198 K, independent of the nature of M^+.

10, 19, 20 to increase from +0.077 to +0.082. With Q = −2.8 mT in the McConnell equation, these values are converted into the coupling constants −0.098, −0.050, and −0.216 mT for the tight ion pairs and −0.087, −0.031, and −0.230 mT for the loose ones, in excellent agreement with their observed counterparts (Table II).

Structure of the Tight Ion Pairs. The hyperfine data in Table II provide several pieces of information on the structure of the tight ion pairs formed by the radical anion $3^{\bullet-}$ with its alkali-metal counterions:

(i) The finding that the protons are throughout equivalent in sets of four indicates that the 2-fold rotational axis perpendicular to the molecular plane must be retained in the ion-paired radical anion, i.e., the counterion must be located on this axis.

(ii) The relatively small absolute values and the negative sign of the coupling constants observed for the alkali-metal nuclei are consistent with the counterion residing in the vertical nodal plane, xz, of the singly occupied orbital b_{3g} (Figure 2). The ratio $|a_{Li}|$:$|a_{Na}|$:$|a_K|$:$|a_{Cs}|$ of 2.1:3.3:1.0:8.4 roughly corresponds to that of the atomic parameters calculated for unit ns-spin population at the Li, Na, K, and Cs atoms.[13] Thus, on going from Li^+ through Na^+ and K^+ to Cs^+, there should be no abrupt change in the structure of the ion pairs.

(13) Morton, J. R.; Preston, K. F. *J. Magn. Reson.* **1978**, *30*, 577.

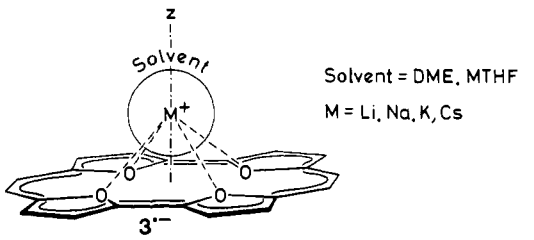

Figure 6. Schematic presentation of the ion pair formed by the radical anion $3^{\bullet-}$ with an alkali-metal counterion M^+.

(iii) The absolute values, $|a_{H\mu}|$, of the perimeter protons smoothly decrease (μ = 2, 7, 12, 17 and 3, 6, 13, 16) or increase (9, 10, 19, 20) in the following order: tight ion pairs, $Li^+ \rightarrow Na^+ \rightarrow K^+ \rightarrow Cs^+ \rightarrow$ loose ion pairs. This order points to a weakening of association between the radical anion and the counterion with the growing size of the alkali-metal cation, as expected for a primary interaction of the counterion with lone electron pairs of the first-row heteroatoms.[14] Such an interaction is also in line with MO calculations, in which the observed trend in the $|a_{H\mu}|$ values has been reproduced by modifying the parameter h_O of the oxygen π-centers (see above).

Summing up, it can be said that the hyperfine data point to a similar C_{2v} structure of all ion pairs, in which the counterion is situated on the 2-fold axis (z) above or below the molecular plane, thus contacting evenly the lone electron pairs of the four oxygen atoms (Figure 6). Although positioning of the counterion in this plane itself is not at variance with the hyperfine data, it can be excluded by comparing the spatial requirement of the oxygen lone pairs[15] and the alkali-metal cations[16] with the dimensions of the rectangular cavity in the tetraoxaporphycenes, as expressed by the X-ray crystallographic O···O distances[3] (3^{2+}, 276 × 261 pm; **3**, 278 × 273 pm). Moreover, a planar $3^{\bullet-}$–M^+ complex of D_{2h} symmetry, which implies a very strong association of the radical anion $3^{\bullet-}$ with its counterion M^+, seems improbable, in view of the reversible change from tight to loose ion pairs in the same solvent (DME), caused just by lowering the temperature.[17] A too close contact of the cation with the lone electron pairs of the oxygen atoms should also be electrostatically disfavored, because, even in the radical anion, these atoms are predicted to bear a positive π-charge population (see below).

UV/Visible/Near-IR Spectra. Figure 7 shows the electronic absorption spectra of the five redox stages, 3^{2+}, $3^{\bullet+}$, **3**, $3^{\bullet-}$, and 3^{2-}, of tetraoxaporphycene in the range 300–950 nm, as well as the emission spectra of the three fluorescent diamagnetic species.[18] The spectrum of the radical anion, $3^{\bullet-}$, could be observed only together with those of the neutral compound **3** and the dianion 3^{2-}, due to the partial disproportionation $2 \times 3^{\bullet-} \rightarrow 3 + 3^{2-}$. The wavelengths of the band maxima are given in Table III.

A feature shared by the charged tetraoxaporphycenes, 3^{2+}, $3^{\bullet+}$, $3^{\bullet-}$, and 3^{2-}, with all porphyrins and porphycenes[1-3,5] is the

(14) First-row heteroatoms with their lone electron pairs are "hard bases" and interact strongly with the "hard acid" Li^+, whereas π-systems represent "soft bases" favoring interaction with the "soft acid" K^+ or Cs^+. See, for example: Fürderer, P.; Gerson, F.; Heinzer, J.; Mazur, S.; Ohya-Nishiguchi, H.; Schroeder, A. H. *J. Am. Chem. Soc.* **1979**, *101*, 2275. Boche, G.; Heidenhain, F. *Angew. Chem., Int. Ed. Engl.* **1978**, *17*, 283.

(15) Lone pairs of electrons are considered to occupy larger volumes than the bonding ones. See, for example: Gillespie, R. J.; Hargittai, I. *The VSEPR Model of Molecular Geometry*; Allyn and Bacon: Boston–London, 1991; Chapter 3.

(16) For radii of alkali-metal cations, see, for example: Pauling, L. *The Nature of the Chemical Bond*, 3rd ed.; Cornell Univ. Press: Ithaca, NY, 1960; Chapter 13.

(17) This statement also holds for Li^+ as the counterion, although a "naked" Li^+ cation (i.e., without a solvent shell at the rear) would fit into the cavity of $3^{\bullet-}$. For a recent paper on the structure of lithium, sodium, and potassium porphyrin complexes, see: Arnold, J.; Dawson, D. Y.; Hoffman, C. G. *J. Am. Chem. Soc.* **1993**, *115*, 2707.

(18) The absorption maxima of 3^{2+} and **3** were reported along with their syntheses.[3] Later on, both absorption and emission spectra of 3^{2+} were presented.[5]

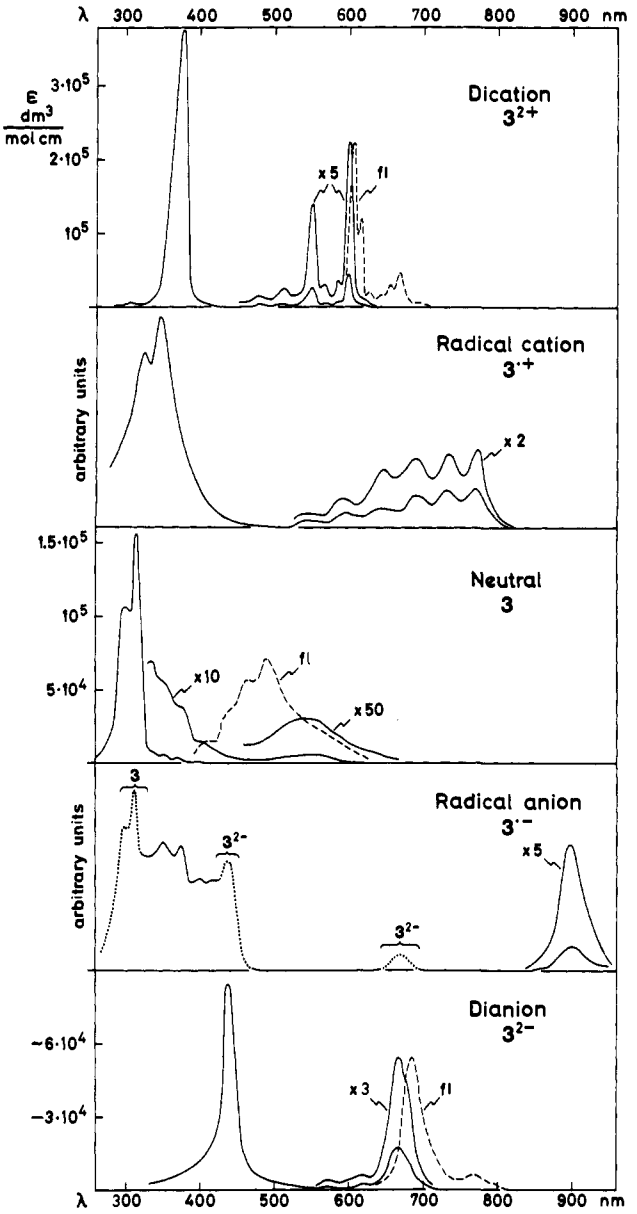

Figure 7. Electronic spectra of the five redox stages of tetraoxaporphycene in the range 300–950 nm. Dication 3^{2+}: solvent, concentrated H_2SO_4; counterion, ClO_4^- (HSO_4^-). Radical cation $3^{\bullet+}$: solvent, DMF; counterion, ClO_4^-. Neutral compound 3: solvent, DME. Radical anion and dianion $3^{\bullet-}$ and 3^{2-}: solvent, DME; counterion, K^+. Temperature: 298 K throughout. In the spectrum of the radical anion $3^{\bullet-}$, the bands drawn by dotted lines stem from the neutral compound 3 or the dianion 3^{2-}. Fluorescence bands (fl) are drawn by dashed lines.

occurrence of two distinct absorption regions: the very strong Soret bands in the UV or the shortwave visible and the less intense Q bands in the visible or the near-IR. The spectra of the four charged tetraoxaporphycenes resemble, in particular, those of the isomeric and isoelectronic tetraoxaporphyrins, 4^{2+}, $4^{\bullet+}$, $4^{\bullet-}$, and 4^{2-}.[6] In both series, the Soret bands lie at 300–400 nm for the dications, radical cations, and radical anions and at 400–450 nm for the dianions. With respect to the corresponding Q bands at 500–950 nm, several comments suggest themselves: (i) The radical anions and dianions absorb at substantially larger wavelengths than their positively charged counterparts, the radical cations and dications. (ii) The bands of the radical ions exhibit a bathochromic shift of ca. 200 nm or 0.5 eV relative to the corresponding diions. (iii) In general, the absorption maxima of the tetraoxaporphycenes appear at somewhat longer waves than those of the analogous tetraoxaporphyrins. The maxima of the Q bands for these charged species can thus be ordered as follows

Table III. Band Maxima (λ in nm)[a] of the Five Redox Stages of Tetraoxaporphycene (3)

	dication 3^{2+}	radical cation $3^{\bullet+}$	neutral 3	radical anion $3^{\bullet-}$	dianion 3^{2-}
abs	307 (w)	330 (vs)	301 (s)	354 (s)	440 (vs)
	376 (vs)	348 (vs)	316 (vs)	378 (s)	567 (w)
	480 (w)	542 (w)	340 (w)	398 (s)	616 (w)
	512 (w)	592 (w)	354 (w)	422 (s)	666 (s)
	550 (s)	646 (w)	375 (w)	902 (s)	
	566 (w)	682 (s)	400 (w)		
	586 (w)	733 (s)	550 (vw)[b]		
	598 (s)	774 (s)			
em	606 (s)		402 (w)		687 (s)
	615 (w)		437 (w)		764 (w)
	627 (w)		462 (w)		
	657 (w)		491 (w)		
	667 (w)				

[a] Experimental error: ±2 nm. Abbreviations: s = strong, w = weak, vs = very strong, vw = very weak, abs = absorption, em = emission. [b] Broad absorption extending from 500 to 600 nm.

(nm): 4^{2+} (524) < 3^{2+} (550 and 598) < 4^{2-} (644) < 3^{2-} (666) < $4^{\bullet+}$ (681) < $3^{\bullet+}$ (733 and 774) < $4^{\bullet-}$ (888) < $3^{\bullet-}$ (902). In the case of the dications and dianions, these bands are reflected by their fluorescence images (nm): 4^{2+} (630), 3^{2+} (606), 4^{2-} (655), and 3^{2-} (687).

The spectra of the neutral tetraoxaporphycene (3) and tetraoxaporphyrin (tetraoxaisophlorin; 4) are also similar. They consist of very strong Soret-like bands at 300–320 nm, followed by several less intense maxima in the adjacent region, 420–490 nm for 4 and 340–400 nm for 3. In addition, these spectra reveal a very weak and broad absorption at longer waves, 600–800 nm for 4 and 500–600 nm for 3. However, the emission band of 3, like that of 4, is not a mirror image of this broad absorption, but its four maxima at 491, 462, 437, and 402 nm (4: 530 and 495 nm) reflect those at 340, 354, 375, and 400 nm (4: 452 and 487 nm) in the region adjacent to the Soret-like band.[19] The similarities in the spectra of 3 and 4, especially the occurrence of the broad absorption in the visible, are noteworthy, because they are in line with the lowering of the symmetry from D_{4h} to D_{2h} postulated for 4 in the previous paper.[6] The hypsochromic shift of this absorption, on passing from 4 to 3, accords with the MO model presented below.

MO Models. In order to assign the electronic bands to transitions between orbitals, MO calculations by the PPP SCF CI method[20] were performed on the three closed-shell systems, 3^{2+}, 3, and 3^{2-}, and they were extended to the two open-shell ones, $3^{\bullet+}$ and $3^{\bullet-}$.[21] In each case, use was made of the five highest occupied and five lowest unoccupied orbitals for configuration interaction.[22] Geometry parameters were available for the dication 3^{2+} and the neutral 3 from their X-ray crystallographic structure analyses.[3] For the radical ions $3^{\bullet+}$ and $3^{\bullet-}$ and the dianion 3^{2-}, the X-ray data of 3^{2+} were preferred to those of 3, because of the distinct bond-length alternation found for the latter and not expected to occur in the charged species. The D_{2h} symmetry was maintained throughout. Figure 8 presents schematically the calculated SCF energy levels of the six relevant

(19) As stated in ref 6, emission bands from the second excited state have been observed for several π-systems with a low-lying first excited state; see: Beer, M.; Longuet-Higgins, H. C. *J. Chem. Phys.* **1955**, *23*, 1390. Dörr, F. In *Optische Anregung organischer Systeme*; Först, W., Ed.; Verlag Chemie: Weinheim, 1965. Wild, U. P.; Griesser, H. J.; Tuan, V. D.; Oth, J. F. M. *Chem. Phys. Lett.* **1976**, *41*, 450. Turro, N. J.; Ramamurthy, V.; Cherry, W.; Farneth, W. *Chem. Rev.* **1978**, *78*, 125. Leupin, W.; Wirz, J. *J. Am. Chem. Soc.* **1980**, *102*, 6068. Leupin, W.; Berens, S. J.; Magde, D.; Wirz, J. *J. Phys. Chem.* **1984**, *88*, 1376.

(20) For a recent publication on the PPP method, see: *Int. J. Quantum Chem.* **1990**, *37*, issue in honor of R. Pariser, R. G. Parr, and J. A. Pople.

(21) The method applied to the open-shell systems followed the theory by Longuet-Higgins and Pople: Longuet-Higgins, H. C.; Pople, J. A. *Proc. Phys. Soc., London* **1955**, *A68*, 591.

(22) Energy heteroatom parameters in electronvolts: $\Delta U(O) = IP(O) - IP(C) = -21.48$; $\beta(C-O) = -2.318$; $\gamma_{\mu\mu} = +22.90$; core charge of O, 2.0.

Table IV. Energies, Intensities, and Compositions of the Electronic Transitions Calculated for the Five Redox Stages of Tetraoxaporphycene (**3**) and Assignments of the Observed Electronic Bands

		ΔE (eV)	ϵ (dm^3 mol^{-1} cm^{-1})	substantial contribution (%)				experiment (λ, nm; ΔE, eV)
dication 3^{2+}	$^1B_{2u} \leftarrow {}^1A_g$ (B_{2u})			$b_{3g} \leftarrow b_{1u}$	$b_{2g} \leftarrow a_u$			
		3.51	1.4×10^5	65	32			376; 3.30
		1.90	5×10^3	32	67			550; 2.25
	$^1B_{3u} \leftarrow {}^1A_g$ (B_{3u})			$b_{2g} \leftarrow b_{1u}$	$b_{3g} \leftarrow a_u$			
		3.66	1.7×10^5	28	59			376; 3.30
		1.83	1.3×10^4	68	31			598; 2.07
radical cation $3^{\bullet+}$	$^2A_u \leftarrow {}^2B_{2g}$ (B_{2u})			$b_{2g} \leftarrow a_u$	$a_u \leftarrow b_{2g}$	$(b_{3g} \leftarrow b_{1u})^\alpha$	$(b_{3g} \leftarrow b_{1u})^\beta$	
		3.69	1.2×10^5	8	17	71	0	348; 3.56
		4.40	10^3	0	31	10	56	*a*
		1.52	5×10^3	90	4	5	0	733; 1.69
		2.09	10^3	1	47	10	41	*a*
	$^2B_{1u} \leftarrow {}^2B_{2g}$ (B_{3u})			$b_{2g} \leftarrow b_{1u}$	$b_{1u} \leftarrow b_{2g}$	$(b_{3g} \leftarrow a_u)^\alpha$	$(b_{3g} \leftarrow a_u)^\beta$	
		3.91	1.3×10^5	7	19	63	0	330; 3.76
		4.33	3×10^3	0	35	7	54	*a*
		1.42	1.1×10^4	91	2	6	0	774; 1.60
		2.51	10^2	0	43	13	41	*a*
neutral **3**	$^1B_{2u} \leftarrow {}^1A_g$ (B_{2u})			$a_u \leftarrow b_{2g}$	$b_{3g} \leftarrow b_{1u}$			
		4.05	5.8×10^4	0	98			301; 4.12
		3.73	5.7×10^4	97	0			340; 3.65
	$^1B_{3u} \leftarrow {}^1A_g$ (B_{3u})			$b_{1u} \leftarrow b_{2g}$	$b_{3g} \leftarrow a_u$			
		4.04	1.1×10^5	62	36			316; 3.92
		3.92	2×10^3	35	62			*a*
	$^1B_{1g} \nleftarrow {}^1A_g$ (B_{1g})			$b_{3g} \leftarrow b_{2g}$	$b_{1u} \leftarrow a_u$	$a_u \leftarrow b_{1u}$		
		2.16	0	96	2	2		~550; ~2.25
radical anion $3^{\bullet-}$	$^2B_{1u} \leftarrow {}^2B_{3g}$ (B_{2u})			$b_{3g} \leftarrow b_{1u}$	$b_{1u} \leftarrow b_{3g}$	$(a_u \leftarrow b_{2g})^\alpha$	$(a_u \leftarrow b_{2g})^\beta$	
		3.44	1.1×10^5	17	7	69	0	378; 3.28
		4.43	9×10^2	40	0	8	49	*a*
		1.56	2×10^3	0	88	8	1	*a*
		2.05	10^3	38	3	11	46	*a*
	$^2A_u \leftarrow {}^2B_{3g}$ (B_{3u})			$b_{3g} \leftarrow a_u$	$a_u \leftarrow b_{3g}$	$(b_{1u} \leftarrow b_{2g})^\alpha$	$(b_{1u} \leftarrow b_{2g})^\beta$	
		3.89	1.2×10^5	8	5	82	1	354; 3.50
		4.32	1.1×10^4	44	1	1	41	*a*
		1.07	1.1×10^4	3	92	4	0	902; 1.37
		2.58	10^2	40	0	10	45	*a*
dianion 3^{2-}	$^1B_{2u} \leftarrow {}^1A_g$ (B_{2u})			$b_{1u} \leftarrow b_{3g}$	$a_u \leftarrow b_{2g}$			
		3.27	1.3×10^5	31	67			440; 2.82
		1.76	9×10^2	68	31			666; 1.86
	$^1B_{3u} \leftarrow {}^1A_g$ (B_{3u})			$a_u \leftarrow b_{3g}$	$b_{1u} \leftarrow b_{2g}$			
		3.66	1.7×10^5	20	79			(440; 2.82)[b]
		1.59	2.4×10^4	79	19			666; 1.86

[a] Not observed or masked by adjacent strong bands. [b] This band at 2.82 eV is the only one which can reasonably be assigned to the predicted strongly allowed transition at 3.66 eV, because the region 250–400 nm (4.96–3.10 eV) is void of noticeable absorption. Although, in general, the PPP SCF CI energies of the Soret bands are markedly higher than their experimental counterparts, a difference as large as 0.8 eV is rather exceptional.

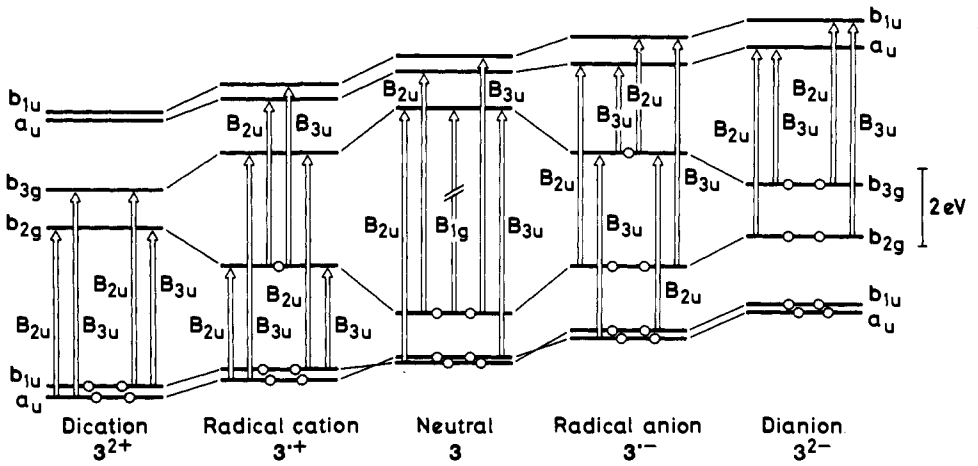

Figure 8. Electronic transitions between SCF energy levels of several highest occupied and lowest unoccupied MOs in the five redox stages of tetraoxaporphycene, as calculated by the PPP method. Instead of using the absolute energy scale, the levels are drawn relative to the center of b_{2g} and b_{3g}. The choice of the axes in the D_{2h} symmetry is specified in Figure 2.

highest occupied or lowest unoccupied orbitals for the five redox stages of tetraoxaporphycene. (These levels do not significantly depend on whether geometry parameters for the dication or the neutral compound were chosen as a starting point in the calculations.) The energy scheme of the four charged species, 3^{2+}, $3^{\bullet+}$, $3^{\bullet-}$, and 3^{2-}, differs from the corresponding diagram[6] of 4^{2+}, $4^{\bullet+}$, $4^{\bullet-}$, and 4^{2-} by the splitting of the degenerate or nearly degenerate orbitals (e_g in the D_{4h} symmetry) into b_{2g} and b_{3g} (D_{2h}), on going from the tetraoxaporphyrin to the tetraoxaporphycene series. In the case of the neutral compounds **3** and **4**, the energy schemes are similar, due to the lowering of the symmetry from D_{4h} to D_{2h} which has been postulated for **4**;[6]

merely, the HOMO (b_{2g})–LUMO (b_{3g}) energy gap is markedly enlarged in **3** relative to **4**.

Assignments of Electronic Bands. As is evident from Figure 8, there are two pairs of symmetry-allowed B_{2u} and B_{3u} transitions in the closed-shell systems, 3^{2+}, **3**, and 3^{2-}, while three such pairs occur in the open-shell ones, $3^{\bullet+}$ and $3^{\bullet-}$. Of the symmetry-forbidden transitions, only that between the HOMO and LUMO in **3** (B_{1g}) is included. Table IV lists the characteristics of all these transitions as calculated by the PPP SCF CI method. The observed bands (Figure 7 and Table III), which have tentatively been assigned to them, are indicated in the last column. The assignments have been guided by comparison of the calculated and observed transition energies (ΔE) and intensities (extinction coefficients ϵ). Agreement between theory and experiment is as good as may be expected considering the size of the extended π-systems and the semiempirical nature of the MO procedure. For the four charged tetraoxaporphycenes, 3^{2+}, $3^{\bullet+}$, $3^{\bullet-}$, and 3^{2-}, this agreement is attained irrespective of the scaling factor used for adapting the parameter β to the bond order.[23] However, for the neutral compound, a serious discrepancy is found when the same value (0.335) has been used for this factor as in the charged species. The calculations then predict four strong B_{2u} and B_{3u} transitions at 4.2–3.9 eV, i.e., in the region of the Soret-like bands at 301 and 316 nm, but they fail to account for the four weaker absorption maxima at the longwave flank of these bands (340–400 nm or 3.65–3.10 eV). As pointed out in a preceding section, the four maxima are faithfully reflected by the emission spectrum, and they must, therefore, represent the vibrational structure of an electronic transition of its own (and not a vibrational progression of the adjacent very intense Soret-like bands). When the scaling factor was reduced (0.195), the "missing" band "appeared" as a B_{2u} transition at 3.73 eV, which compares favorably with an observed maximum at 340 nm (3.65 eV). This modification in the PPP program leads to a lowering in the energy of the forbidden B_{1g} transition from 2.47 to 2.16 eV (the observed broad absorption is centered at ca. 550 nm or 2.25 eV). The values thus calculated for **3** are given in Table IV instead of those obtained with the higher scaling factor.

π-Bond Orders and π-Charge Populations. As indicated in Figure 9, the π-bond orders calculated by the PPP SCF CI method[20,22] for the 20-membered perimeter in the tetraoxaporphycene diions 3^{2+} (0.55–0.73) and 3^{2-} (0.51–0.67) point to a substantial π-delocalization along this perimeter, whereas the neutral compound **3** should be regarded as consisting of four furan moieties and two ethene π-systems linked by "essential single bonds" (order 0.32–0.34). The structural features, bond equalization in the diions and alternation of single and double bonds in the neutral compound, are shared with corresponding tetraoxaporphyrins 4^{2+}, 4^{2-}, and **4**,[6] albeit with the alternation being, expectedly, more pronounced in **3** than in **4**.

Also shown in Figure 9 are the calculated π-charge populations in 3^{2+}, **3**, and 3^{2-}. The four oxygen atoms in 3^{2+} bear one positive π-charge (+0.25 × 4), the second one being distributed among the 20 π-centers of the perimeter. The tetraoxaporphycene dication, 3^{2+}, can thus be adequately represented by three mesomeric formulas depicted in Figure 10. The π-charge populations at the oxygen atoms remain unchanged or decrease only slightly on passing to the neutral **3** (+0.25) and the dianion 3^{2-} (+0.20), so that admission of additional electrons to 3^{2+} should almost exclusively affect the 20-membered π-perimeter. This

(23) In our PPP calculations for closed shells, the parameter $\beta_{\mu\nu}$ was iteratively adjusted to the bond order $p_{\mu\nu}$ within each SCF cycle by using the formula $\beta_{\mu\nu} = \beta_0 \exp[s(p_{\mu\nu}-2/3)]$, where s is the scaling factor.

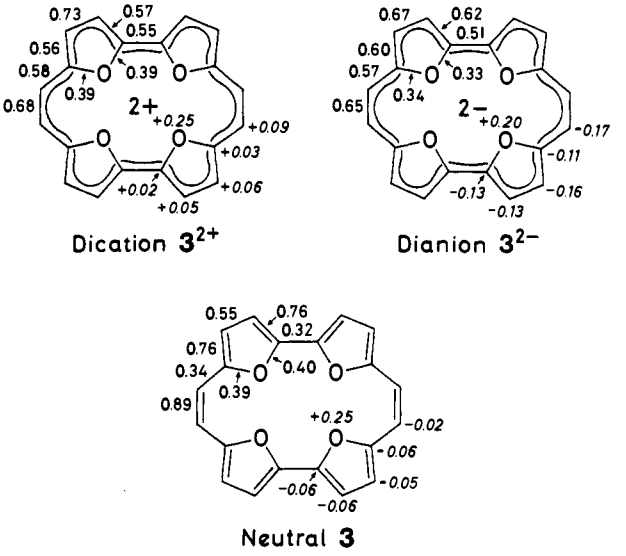

Figure 9. π-Bond orders (upper halves of the formulas) and π-charge populations (lower halves of the formulas, in italics) of tetraoxaporphycene diions 3^{2+} and 3^{2-} and the neutral compound **3**, as calculated by the PPP method.

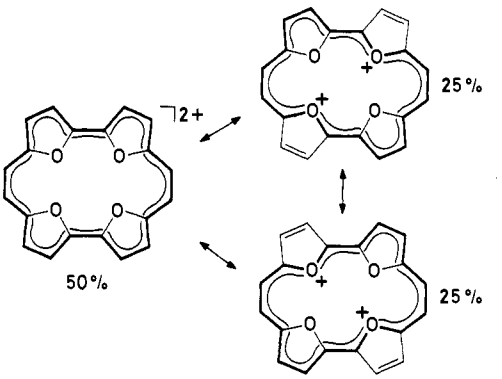

Figure 10. Mesomeric formulas of the tetraoxaporphycene dication, 3^{2+}.

π-charge distribution in 3^{2+}, **3**, and 3^{2-} strongly resembles that in the corresponding redox stages of tetraoxaporphyrin,[6] 4^{2+}, **4**, and 4^{2-}.

The π-bond orders and π-charge populations calculated for the radical ions by the open-shell method[21] (not indicated in Figure 9) are intermediate between those of 3^{2+} and **3** for $3^{\bullet+}$ and between 3^{2-} and **3** for $3^{\bullet-}$.

Concluding Remarks

Despite changes in the shape and symmetry ($D_{4h} \rightarrow D_{2h}$), the basic π-electronic structure is essentially maintained not only on going from porphyrins to porphycenes[2,5] but also on passing from the five stages of tetraoxaporphyrin[6] to those of tetraoxaporphycene. Such a conclusion can be drawn from the spectroscopic and other physical and chemical properties which primarily depend on the π-electron distribution. Evidently, these properties are mainly determined by the same number of π-electrons and similar cyclic π-delocalization in all systems in question.

Acknowledgment. This work was supported by the Swiss National Science Foundation. We thank Professor J. Wirz (Basel) for the permission to use his optical spectrometers.